Research Paper
Computational Methods for Differential Equations
http://cmde.tabrizu.ac.ir
Vol. *, No. *, *, pp. 1-10
DOI:10.22034/cmde.2025.64151.2889

Analysis of blood sugar with an incomplete ℵ-function

Manisha Meena*

Department of Mathematics, Motilal Nehru College, University of Delhi, Delhi, India.

Abstract

Mathematical modeling plays a vital role in understanding complex medical and biological processes. In this study, we develop a mathematical model incorporating the incomplete ℵ-function to analyze glucose supply in human blood. The model provides a generalized framework to assess glucose dynamics under varying physiological conditions. Numerical simulations demonstrate the impact of key parameters on glucose distribution, revealing critical thresholds for maintaining optimal glucose levels. The findings offer valuable insights into glucose regulation mechanisms, with potential applications in diabetes management and metabolic health monitoring. The general results reveal several intriguing cases concerning the relevant parameters involved.

Keywords. Sumudu Transform, Glucose Tolerance Test, Mellin-Barnes Type Integral, Incomplete ℵ-Function.
2010 Mathematics Subject Classification. 30E20, 33C60, 92C99.

1. Introduction

Over the past forty years, mathematicians and scientists have been increasingly captivated by fractional calculus and special functions due to their extensive applications and importance in diverse fields such as computer science, biological science, medical science, ecology, control theory, social sciences, diffusive transport, electrical finance networks, viscoelasticity, signal processing, fluid dynamics, and environmental science [6, 26]. The incomplete ℵ-function has been identified in numerous response-related problems, reaction-diffusion, encompassing diffusion, connectivity, and electronics fractional differential equations, as well as other domains of physics, probability theory, biology [17, 27].

Fractional calculus has emerged as a powerful tool for modeling complex dynamical systems, particularly in biological and epidemiological studies. Recent advancements highlight its applicability in diverse areas, including disease modeling, population dynamics, and physiological processes. Bhatter et al. [6] explored the Srivastava-Luo-Raina M-transform involving incomplete I-functions, providing a robust mathematical framework for fractional calculus. The study by Higazy et al. [15] examined the structural properties of a generalized Caputo fractional-order Lotka-Volterra system, demonstrating its efficiency in capturing memory effects. In epidemiology, Panwar et al. [21] analyzed a nonlinear smoking model using fractional operators, while El-Mesady and Ali [**?**] investigated the role of preventive measures in a fractional-order chickenpox model. Fractional models have also been instrumental in understanding COVID-19 transmission, as illustrated by Adel et al. [1], who incorporated lockdown effects into a novel fractional framework. Additionally, Elsonbaty et al. [14] proposed a discrete fractional model for lumpy skin disease, while El-Mesady et al. [**?**] explored its nonlinear dynamics and control strategies. Beyond epidemiology, Shyamsunder [25] provided a comparative analysis of fractional models for blood alcohol concentration, emphasizing their numerical efficiency. Furthermore, El-Mesady et al. [**?**] presented a fractional-order vaccination model for tuberculosis, incorporating susceptible individuals with underlying ailments. These studies collectively underscore the versatility of fractional calculus in modeling real-world phenomena, motivating its application in glucose dynamics within the human body.

Received: 22 October 2024 ; Accepted: 12 August 2025.
∗ Corresponding author. Email: math.manisha96@gmail.com.

The human body is made up of several organs, each of which has a distinct purpose that is necessary to sustain biological activity. These cellular processes depend on a steady and continuous supply of glucose. Thus, maintaining optimal blood glucose levels is important: Hypoglycemia affects the ability of organs to function normally, whereas hyperglycemia causes glucotoxicity. Under typical metabolic conditions, the human body is designed to maintain blood glucose levels between 80 and 120 mg/dL [7, 18]. Glycaemia is a term used to describe the amount of glucose in human blood. It is often referred to as blood glucose level or blood glucose concentration. About 4 grammes of glucose circulate in the blood of a 70 kg person on average [35]. Even while glucose makes up a very little portion of the body's mass, many different types of cells are sensitive to its presence and rely on it. Considering the significance of these 4 grammes of glucose, a complex regulatory mechanism is in place to ensure stable blood sugar levels. Our comprehension of this regulatory system has been substantially enhanced by experiments conducted on a variety of tissues, cells, and organs. It is amazing how well the body can provide dietary glucose while preserving blood glucose homeostasis.

Although the kidney can produce glucose, it is a far less significant source than the liver. Ingesting a high-carbohydrate meal increases insulin secretion from cells, which promotes glucose removal from the blood into the muscles, liver, and fat while inhibiting glucose release from the liver into the bloodstream. This reduces fluctuations in blood sugar levels. During exercise, insulin-independent mechanisms that increase glucose uptake in the muscles are activated, and the liver produces glucose to stabilize blood sugar levels. Hypoglycemia occurs when glucose production does not increase, often due to excessive insulin in people with diabetes. Severe hypoglycemia can lead to neuroglycopenia, seizures, metabolic dysfunction, and death. Persistent hyperglycemia leads to "glucose poisoning," contributing to diabetes complications such as β-cell dysfunction and pathology. Alcohol consumption initially raises blood sugar levels, which subsequently drop, and some medications can also affect glucose levels [**?**].

The process known as glycogenesis transforms excess glucose into glycogen, which is then stored in the muscle and liver cells. When blood sugar levels drop, glycogenolysis and gluconeogenesis restore glucose levels to normal. Stored glycogen in the muscles and liver is converted by glycogenolysis first to glucose-1-phosphate and subsequently to glucose-6-phosphate. Synthesis of glucose from non-carbohydrate sources is known as gluconeogenesis. Together, these metabolic mechanisms keep blood sugar levels within acceptable ranges. However, the time required for these processes is shorter for an average person and longer for someone with diabetes. Various methods exist to test and measure blood sugar levels, including the glucose tolerance test, which assesses how effectively the body processes glucose by measuring blood sugar at specific intervals after glucose consumption. This test plays a crucial role in diagnosing diabetes and prediabetes. For an in-depth mathematical analysis of these methods, see Kapur's 1985 study [19].

Despite significant advancements in mathematical modeling of glucose regulation, existing models often fail to capture the intricate dynamics of glucose homeostasis influenced by physiological and external factors. Most conventional models rely on classical differential equations, which may not adequately describe glucose metabolism's memory and hereditary properties. Furthermore, the role of special functions in modeling glucose dynamics remains under explored. To address these gaps, this study introduces a novel mathematical model incorporating the incomplete $\aleph$-function, offering a more generalized and flexible framework for analyzing blood glucose levels [2, 8]. Unlike existing approaches, this model enables a more comprehensive examination of glucose fluctuations by leveraging fractional-order derivatives and special functions. Through numerical simulations, we investigate the impact of key physiological parameters, identifying critical thresholds that influence glucose regulation. The insights derived from this study provide a deeper understanding of glucose metabolism and offer potential applications in biomedical science, personalized medicine, and metabolic disorder management [28, 29].

The remainder of this paper is structured as follows: Section 2 presents the necessary mathematical preliminaries and foundational concepts. In section 3, we discuss the main findings of our study, highlighting key theoretical results. Section 4 provides a graphical discussion, illustrating the impact of various parameters through numerical simulations. Finally, section 5 concludes the study by summarizing the findings and outlining potential future research directions, followed by a list of references.

2. Preliminaries

This part will present some basic definitions and formulas that we will discuss in the study.

Definition 2.1. Consider $\wp(t)$ a real-valued integrable function. Then, the fractional derivative of order $0 < \mathrm{a} < 1$ in the Caputo sense is defined as follows [20]:

$$ {}^{C}D_t^{\mathrm{a}}(\wp(t)) = \frac{1}{\Gamma(r-\mathrm{a})}\int_0^t \frac{\wp^r(w)}{(t-w)^{\mathrm{a}-r+1}}\, dw, \tag{2.1}$$

where $r = [\mathrm{a}] + 1$.

Definition 2.2. Consider the set $\mathbb{S}$ as described in [**?**].

$$\mathbb{S} = \{\ \varphi(z) : \exists\ \mathbf{M}, \alpha_1, \alpha_2 > 0, |\varphi(z)| < \mathbf{M}e^{\frac{|z|}{\alpha_i}},\ if\ z \in (-1)^i \times [0,\infty)\},$$

for all real $z \geq 0$, the Sumudu transform (ST) of a function $\varphi(z) \in \mathbb{S}$ is given by $\mathcal{S}[\varphi(z)] = \Phi(K)$;

$$\mathcal{S}[\varphi(z); K] = \Phi(K) = \int_0^\infty e^{-z}\varphi(Kz)dz \quad ; \quad K \in (-\alpha_1, \alpha_2).$$

The inversion formula for the ST is expressed as

$$\mathcal{S}^{-1}[\Phi(K); z] = \varphi(z) = \frac{1}{2\pi i}\int_{\varpi - i\infty}^{\varpi + i\infty} e^{Kz}\Phi\Big(\frac{1}{K}\Big)\frac{dK}{K},$$

where $\varpi \in \mathbb{R}$ is a constant.

Definition 2.3. The ST of Equation (2.1) is provided as follows [**?**]:

$$\mathcal{S}[{}^{C}D_t^{\mathrm{a}}\,\wp(t); K] = \frac{\mathcal{S}[\wp(t)] - \wp(0)}{K^{\mathrm{a}}}.$$

Incomplete Gamma Function: The standard incomplete gamma functions $\gamma(\mathfrak{g}, \zeta)$ and $\Gamma(\mathfrak{g}, \zeta)$ are represented as [**?**]:

$$\gamma(\mathfrak{g}, \zeta) := \int_0^\zeta \theta^{\mathfrak{g}-1}\, e^{-\theta}\, d\theta, \qquad \big(\Re(\mathfrak{g}) > 0;\ \zeta \geq 0\big),$$

and

$$\Gamma(\mathfrak{g}, \zeta) := \int_\zeta^\infty \theta^{\mathfrak{g}-1}\, e^{-\theta}\, d\theta, \qquad \big(\Re(\mathfrak{g}) > 0;\ \zeta \geq 0\big),$$

satisfy the subsequent decomposition rule:

$$\gamma(\mathfrak{g}, \zeta) + \Gamma(\mathfrak{g}, \zeta) := \Gamma(\mathfrak{g}), \qquad \big(\Re(\mathfrak{g}) > 0\big),$$

where $\Re(\mathfrak{g})$ denotes the real part of the parameter $\mathfrak{g}$.

Furthermore, when we set $\zeta = 0$, we obtain $\Gamma(\mathfrak{g}, \zeta) = \Gamma(\mathfrak{g})$.

Aleph Function: The $\aleph$-function, which is a general higher transcendental function introduced by Sudland et al. in their works, specifically in [32, 33], is formally defined as follows:

$$\begin{aligned}\aleph(\varrho) &= \aleph^{u,v}_{r_l,\, s_l,\, f_l;\, \wp}\left[\varrho \,\middle|\, \begin{matrix}(\Theta_m, \mathfrak{E}_m)_{1,v},\ [f_m(\Theta_{ml}, \mathfrak{E}_{ml})]_{v+1,r_l} \\ (\mathcal{Q}_m, \mathcal{B}_m)_{1,u},\ [f_m(\mathcal{Q}_{ml}, \mathcal{B}_m)]_{u+1,s_l}\end{matrix}\right] \\ &= \frac{1}{2\pi\iota}\int_{\$} \Omega(\mathbf{w})\ \varrho^{-\mathbf{w}}\, d\mathbf{w},\end{aligned}$$

where $\varrho \in \mathbb{C}/0$, $\iota = \sqrt{-1}$, and

$$\Omega(\mathbf{w}) = \frac{\prod_{m=1}^{u} \Gamma(\mathcal{Q}_m + \mathcal{B}_m \mathbf{w}) \prod_{m=1}^{v} \Gamma(1 - \Theta_m - \mathfrak{E}_m \mathbf{w})}{\sum_{l=1}^{\wp} f_l \Big[\prod_{m=u+1}^{s_l} \Gamma(1 - \mathcal{Q}_{ml} - \mathcal{B}_m \mathbf{w}) \prod_{m=v+1}^{r_l} \Gamma(\Theta_{ml} + \mathfrak{E}_{ml} \mathbf{w}) \Big]}.$$

The integral path $\$ = \$_{\iota\gamma\infty}\, (\gamma \in \mathbb{R})$ extends from $\gamma - \iota\infty$ and $\gamma + \iota\infty$; the poles of gamma function $\Gamma(1 - \Theta_m - \mathfrak{E}_m \mathbf{w})\, (m = 1, \cdots, v)$ do not exactly match with the poles of gamma function $\Gamma(\mathcal{Q}_m + \mathcal{B}_m \mathbf{w})\, (m = 1, \cdots, u)$; the parameters r_l, s_l are non-negative integers satisfying $0 \leq v \leq r_l$ and $1 \leq u \leq s_l$ for $l = 1, \cdots, r$; $\mathfrak{E}_m$, $\mathcal{B}_m$, $\mathfrak{E}_{ml}$, $\mathcal{B}_{ml}$ are positive real numbers, and Θ_m, $\mathcal{Q}_m$, Θ_{ml}, $\mathcal{Q}_{ml}$ are complex and the empty product is interpreted as unity. For the existence conditions and further details of ℵ-function one can refer to [32].

Incomplete ℵ-Function: The incomplete ℵ-functions ${}^{\gamma}\aleph^{u,v}_{r_l,\, s_l,\, f_l;\, \wp}(\varrho)$ and ${}^{\Gamma}\aleph^{u,v}_{r_l,\, s_l,\, f_l;\, \wp}(\varrho)$ containig the incomplete gamma functions $\gamma(\mathfrak{g}, \zeta)$ and $\Gamma(\mathfrak{g}, \zeta)$ introduced by Bansal et al. [**?**] as define below:

$$\begin{aligned} {}^{\gamma}\aleph^{u,v}_{r_l,\, s_l,\, f_l;\, \wp}(\varrho) &= {}^{\gamma}\aleph^{u,v}_{r_l,\, s_l,\, f_l;\, \wp}\left[\varrho \,\middle|\, \begin{matrix} (\Theta_1, \mathfrak{E}_1 : z), (\Theta_m, \mathfrak{E}_m)_{2,v}, [f_m(\Theta_{ml}, \mathfrak{E}_{ml})]_{v+1,r_l} \\ (\mathcal{Q}_m, \mathcal{B}_m)_{1,u}, [f_m(\mathcal{Q}_{ml}, \mathcal{B}_m)]_{u+1,s_l} \end{matrix}\right] \\ &= \frac{1}{2\pi\iota} \int_{\$} \mathfrak{w}(\mathbf{w}, z)\, \varrho^{-\mathbf{w}}\, d\mathbf{w}, \end{aligned} \tag{2.2}$$

and

$$\begin{aligned} {}^{\Gamma}\aleph^{u,v}_{r_l,\, s_l,\, f_l;\, \wp}(\varrho) &= {}^{\Gamma}\aleph^{u,v}_{r_l,\, s_l,\, f_l;\, \wp}\left[\varrho \,\middle|\, \begin{matrix} (\Theta_1, \mathfrak{E}_1 : z), (\Theta_m, \mathfrak{E}_m)_{2,v}, [f_m(\Theta_{ml}, \mathfrak{E}_{ml})]_{v+1,r_l} \\ (\mathcal{Q}_m, \mathcal{B}_m)_{1,u}, [f_m(\mathcal{Q}_{ml}, \mathcal{B}_m)]_{u+1,s_l} \end{matrix}\right] \\ &= \frac{1}{2\pi\iota} \int_{\$} \Psi(\mathbf{w}, z)\, \varrho^{-\mathbf{w}}\, d\mathbf{w}, \end{aligned} \tag{2.3}$$

where

$$\Psi(\mathbf{w}, z) = \frac{\gamma(1 - \Theta_1 - \mathfrak{E}_1 \mathbf{w}; z) \prod_{m=1}^{u} \Gamma(\mathcal{Q}_m + \mathcal{B}_m \mathbf{w}) \prod_{m=2}^{v} \Gamma(1 - \Theta_m - \mathfrak{E}_m \mathbf{w})}{\sum_{l=1}^{\wp} f_l \Big[\prod_{m=u+1}^{s_l} \Gamma(1 - \mathcal{Q}_{ml} - \mathcal{B}_m \mathbf{w}) \prod_{m=v+1}^{r_l} \Gamma(\Theta_{ml} + \mathfrak{E}_{ml} \mathbf{w}) \Big]},$$

$$\mathfrak{w}(\mathbf{w}, z) = \frac{\Gamma(1 - \Theta_1 - \mathfrak{E}_1 \mathbf{w}; z) \prod_{m=1}^{u} \Gamma(\mathcal{Q}_m + \mathcal{B}_m \mathbf{w}) \prod_{m=2}^{v} \Gamma(1 - \Theta_m - \mathfrak{E}_m \mathbf{w})}{\sum_{l=1}^{\wp} f_l \Big[\prod_{m=u+1}^{s_l} \Gamma(1 - \mathcal{Q}_{ml} - \mathcal{B}_m \mathbf{w}) \prod_{m=v+1}^{r_l} \Gamma(\Theta_{ml} + \mathfrak{E}_{ml} \mathbf{w}) \Big]}, \tag{2.4}$$

for $\varrho \neq 0$, $z \geq 0$, the incomplete ℵ-functions ${}^{\gamma}\aleph^{u,v}_{r_l,\, s_l,\, f_l;\, \wp}(\varrho)$ and ${}^{\Gamma}\aleph^{u,v}_{r_l,\, s_l,\, f_l;\, \wp}(\varrho)$ in (2.2) and (2.3) exist under conditions [**?**]. Such as

$$\delta_l > 0,\ |arg(\varrho)| < \tfrac{1}{2}\delta\pi, \quad l = 1, \cdots, \wp.$$

$$\delta_l > 0,\ |arg(\varrho)| < \tfrac{1}{2}\delta\pi, \quad \text{and} \quad \Re(\Delta)_l + 1 < 0,$$

where

$$\delta_l = \sum_{m=1}^{v} \mathfrak{E}_m + \sum_{m=1}^{u} \mathcal{B}_m - f_l\Big(\sum_{m=v+1}^{r_l} \mathfrak{E}_{ml} + \sum_{m=u+1}^{s_l} \mathcal{B}_{ml} \Big),$$

$$\Delta_l = \sum_{m=1}^{u} \mathcal{Q}_m - \sum_{m=1}^{v} \Theta_m + f_l\Big(\sum_{m=u+1}^{s_l} \mathfrak{E}_{ml} - \sum_{m=v+1}^{r_l} \mathcal{B}_{ml} \Big) + \frac{1}{2}(r_l - s_l), \quad l = 1, \cdots, \wp. \tag{2.5}$$

The incomplete ℵ-functions ${}^{\gamma}\aleph^{u,v}_{r_l,\,s_l,\,f_l;\,\wp}(\varrho)$ and ${}^{\Gamma}\aleph^{u,v}_{r_l,\,s_l,\,f_l;\,\wp}(\varrho)$ defined in (2.2) and (2.3), simplified to numereous special functions such as ℵ-function, incomplete I-functions [**?**], I-functions [**?**], incomplete H-functions, Fox's H-function, etc.

3. Main Findings

The Sumudu integral transform technique has been employed as a robust mathematical tool to address the problem, effectively converting complex differential equations into algebraic forms. This transformation enhances computational efficiency while maintaining the problem's original domain, allowing for high-accuracy solutions. A mathematical model utilizing incomplete ℵ-functions, a specialized class of functions dependent on a single variable, has been formulated to quantify glucose absorption into the bloodstream. These incomplete ℵ-functions effectively capture the dynamic behavior of glucose metabolism, requiring careful evaluation concerning specified variables and parameters for precise glucose supply estimation.

Theorem 3.1. *Let φ be a function satisfying the conditions stated in $\mathbb{S}$, and consider the incomplete ℵ-function representation of the glucose supply model. Then, the generalized form of the function is given by:*

$$
\begin{aligned}
{}^{\gamma}\aleph^{u+1,v}_{r_l,\,s_l,\,f_l;\,\wp}(\varrho) &= {}^{\gamma}\aleph^{u+1,v}_{r_l+1,\,s_l+1,\,f_l;\,\wp}\left[\varrho\,\middle|\,\begin{matrix}(\Theta_1,\mathfrak{E}_1:z),(1+\varrho;\varrho_1),(\Theta_m,\mathfrak{E}_m)_{2,v},\,[f_m(\Theta_{ml},\mathfrak{E}_{ml})]_{v+1,r_l}\\ (\varrho,\varrho_1),(\mathcal{Q}_m,\mathcal{B}_m)_{1,u},\,[f_m(\mathcal{Q}_{ml},\mathcal{B}_m)]_{u+1,s_l}\end{matrix}\right]\\
&= \frac{\tau^{\vartheta-1}\varphi}{\Gamma(\vartheta+1)}\Big(\alpha-\frac{\tau\varphi}{(1+\vartheta)}\Big)\\
&\times {}^{\gamma}\aleph^{u+1,v}_{r_l+1,\,s_l+1,\,f_l;\,\wp}\left[\varrho\,\middle|\,\begin{matrix}(\Theta_1,\mathfrak{E}_1:z),(1+\tau,\tau_1),(\Theta_m,\mathfrak{E}_m)_{2,v},\,[f_m(\Theta_{ml},\mathfrak{E}_{ml})]_{v+1,r_l}\\ (\tau,\tau_1),(\mathcal{Q}_m,\mathcal{B}_m)_{1,u},\,[f_m(\mathcal{Q}_{ml},\mathcal{B}_m)]_{u+1,s_l}\end{matrix}\right]\\
&+ \Lambda\,{}^{\gamma}\aleph^{u,v}_{r_l,\,s_l,\,f_l;\,\wp}\left[\varrho\,\middle|\,\begin{matrix}(\Theta_1,\mathfrak{E}_1:z),(\Theta_m,\mathfrak{E}_m)_{2,v},\,[f_m(\Theta_{ml},\mathfrak{E}_{ml})]_{v+1,r_l}\\ (\mathcal{Q}_m,\mathcal{B}_m)_{1,u},\,[f_m(\mathcal{Q}_{ml},\mathcal{B}_m)]_{u+1,s_l}\end{matrix}\right]
\end{aligned}
\tag{3.1}
$$

with δ_l and Δ_l define by (2.5)

(i) $\tau>\tau_1,\varrho>\varrho_1$,
(ii) $z\geq 0,\varphi$ *is proportional constant,*
(iii) $\delta_l>0,\ |arg(\varrho)|<\frac{1}{2}\delta\pi,\quad l=1,\cdots,\wp,$
(iv) $\delta_l>0,\ |arg(\varrho)|<\frac{1}{2}\delta\pi,\quad$ *and* $\quad\Re(\Delta)_l+1<0.$

Proof. Compartment that continuously supplies the blood with glucose at a rate φ. The following formula will be used to express the blood glucose level at any given time τ, $\varrho(\tau)$ ([23], pp. 65, (2.1)):

$$\frac{d\varrho}{d\tau}=-\varphi(\varrho-\alpha),$$

where φ is the proportionality constant, often known as the transfer coefficient.

The above differential equation in Caputo sense is obtained as follows:

$${}^{C}D^{\vartheta}_{\tau}\varrho=-\varphi(\varrho-\alpha).$$

After taking Sumudu transform, we have

$$\varrho(S)=\Lambda+S^{\vartheta}\varphi\alpha-\varphi S^{\vartheta+1},$$

where $\varrho(0)=\Lambda$ is constant.

Further taking inverse Sumudu transform, we have

$$\varrho=\Lambda+\frac{\tau^{\vartheta}\varphi\alpha}{\Gamma(\vartheta+1)}-\frac{\tau^{\vartheta+1}\varphi}{\Gamma(\vartheta+2)},$$

$$\frac{\Gamma(\varrho+1)}{\Gamma(\varrho)}=\Lambda+\frac{\tau^{\vartheta-1}\varphi\alpha\Gamma(\tau+1)}{\Gamma(\vartheta+1)\Gamma(\tau)}-\frac{\tau^{\vartheta}\varphi\Gamma(\tau+1)}{\Gamma(\vartheta+2)\Gamma(\tau)},\tag{3.2}$$

It is assumed that φ depends on τ. It is possible to think of this transfer coefficient as the rate at which the amount of sugar varies for every unit.

Again, put $\varrho = \varrho - \varrho_1 \mathbf{w}$, $\tau = \tau - \tau_1 \mathbf{w}$ (since as time increases, the level of glucose will decrease) in (3.2).

Multiplying both sides of (3.2) by $\frac{1}{2\pi\iota}\mathfrak{w}(\mathbf{w}, z)\varrho^{\mathbf{w}}$ where $\mathfrak{w}(\mathbf{w}, z)$ defined in Equation (2.4) and on integrating both sides with respect to w in the direction of contour \$ and using (2.3), we obtain the desired result (3.1). □

Likewise, we can solve using the lower incomplete ℵ-function denoted as ${}^{\gamma}\aleph^{u,v}_{r_l,\, s_l,\, f_l;\, \wp}$.

Corollary 3.2. *The following image formulas exist for the ℵ-function [32, 33] if $z = 0$ is set to (3.1):*

$$\aleph^{u+1,v}_{r_l+1,\, s_l+1,\, f_l;\, \wp}\left[\varrho\middle|\begin{matrix}(\Theta_1, \mathfrak{E}_1 : 0), (1+\varrho; \varrho_1), (\Theta_m, \mathfrak{E}_m)_{2,v}, [f_m(\Theta_{ml}, \mathfrak{E}_{ml})]_{v+1,r_l} \\ (\varrho, \varrho_1), (\mathcal{Q}_m, \mathcal{B}_m)_{1,u}, [f_m(\mathcal{Q}_{ml}, \mathcal{B}_m)]_{u+1,s_l}\end{matrix}\right]$$
$$= \frac{\tau^{\vartheta-1}\varphi}{\Gamma(\vartheta+1)}\left(\alpha - \frac{\tau\varphi}{(1+\vartheta)}\right)\aleph^{u+1,v}_{r_l+1,\, s_l+1,\, f_l;\, \wp}\left[\varrho\middle|\begin{matrix}(1+\tau, \tau_1), (\Theta_m, \mathfrak{E}_m)_{1,v}, [f_m(\Theta_{ml}, \mathfrak{E}_{ml})]_{v+1,r_l} \\ (\tau, \tau_1), (\mathcal{Q}_m, \mathcal{B}_m)_{1,u}, [f_m(\mathcal{Q}_{ml}, \mathcal{B}_m)]_{u+1,s_l}\end{matrix}\right]$$
$$+ \Lambda\,\aleph^{u,v}_{r_l,\, s_l,\, f_l;\, \wp}\left[\varrho\middle|\begin{matrix}(\Theta_m, \mathfrak{E}_m)_{1,v}, [f_m(\Theta_{ml}, \mathfrak{E}_{ml})]_{v+1,r_l} \\ (\mathcal{Q}_m, \mathcal{B}_m)_{1,u}, [f_m(\mathcal{Q}_{ml}, \mathcal{B}_m)]_{u+1,s_l}\end{matrix}\right]. \tag{3.3}$$

Corollary 3.3. *When $f_l = 1$ is entered in the main result (3.1), the incomplete I-function proposed by Bansal and Kumar [4] may be represented by the following image formula:*

$${}^{\Gamma}I^{u+1,v}_{r_l+1,\, s_l+1,\, 1;\, \wp}\left[\varrho\middle|\begin{matrix}(\Theta_1, \mathfrak{E}_1 : z), (1+\varrho; \varrho_1), (\Theta_m, \mathfrak{E}_m)_{2,v}, [1(\Theta_{ml}, \mathfrak{E}_{ml})]_{v+1,r_l} \\ (\varrho, \varrho_1), (\mathcal{Q}_m, \mathcal{B}_m)_{1,u}, [1(\mathcal{Q}_{ml}, \mathcal{B}_m)]_{u+1,s_l}\end{matrix}\right]$$
$$= \frac{\tau^{\vartheta-1}\varphi}{\Gamma(\vartheta+1)}\left(\alpha - \frac{\tau\varphi}{(1+\vartheta)}\right){}^{\Gamma}I^{u+1,v}_{r_l+1,\, s_l+1;\, \wp}\left[\varrho\middle|\begin{matrix}(\Theta_1, \mathfrak{E}_1 : z), (1+\tau, \tau_1), (\Theta_m, \mathfrak{E}_m)_{2,v}, (\Theta_{ml}, \mathfrak{E}_{ml})_{v+1,r_l} \\ (\tau, \tau_1), (\mathcal{Q}_m, \mathcal{B}_m)_{1,u}, (\mathcal{Q}_{ml}, \mathcal{B}_m)_{u+1,s_l}\end{matrix}\right]$$
$$+ \Lambda\,{}^{\Gamma}I^{u,v}_{r_l,\, s_l;\, \wp}\left[\varrho\middle|\begin{matrix}(\Theta_1, \mathfrak{E}_1 : z), (\Theta_m, \mathfrak{E}_m)_{2,v}, (\Theta_{ml}, \mathfrak{E}_{ml})_{v+1,r_l} \\ (\mathcal{Q}_m, \mathcal{B}_m)_{1,u}, (\mathcal{Q}_{ml}, \mathcal{B}_m)_{u+1,s_l}\end{matrix}\right]. \tag{3.4}$$

Corollary 3.4. *When $z = 0$ and $f_l = 1$ are set once more in (3.1), the image formula for the I-function proposed by Saxena [24] exists:*

$$I^{u+1,v}_{r_l+1,\, s_l+1,\, 1;\, \wp}\left[\varrho\middle|\begin{matrix}(\Theta_1, \mathfrak{E}_1 : 0), (1+\varrho; \varrho_1), (\Theta_m, \mathfrak{E}_m)_{2,v}, [1(\Theta_{ml}, \mathfrak{E}_{ml})]_{v+1,r_l} \\ (\varrho, \varrho_1), (\mathcal{Q}_m, \mathcal{B}_m)_{1,u}, [1(\mathcal{Q}_{ml}, \mathcal{B}_m)]_{u+1,s_l}\end{matrix}\right]$$
$$= \frac{\tau^{\vartheta-1}\varphi}{\Gamma(\vartheta+1)}\left(\alpha - \frac{\tau\varphi}{(1+\vartheta)}\right)I^{u+1,v}_{r_l+1,\, s_l+1;\, \wp}\left[\varrho\middle|\begin{matrix}(1+\tau, \tau_1), (\Theta_m, \mathfrak{E}_m)_{1,v}, (\Theta_{ml}, \mathfrak{E}_{ml})_{v+1,r_l} \\ (\tau, \tau_1), (\mathcal{Q}_m, \mathcal{B}_m)_{1,u}, (\mathcal{Q}_{ml}, \mathcal{B}_m)_{u+1,s_l}\end{matrix}\right]$$
$$+ \Lambda\, I^{u,v}_{r_l,\, s_l;\, \wp}\left[\varrho\middle|\begin{matrix}(\Theta_m, \mathfrak{E}_m)_{1,v}, (\Theta_{ml}, \mathfrak{E}_{ml})_{v+1,r_l} \\ (\mathcal{Q}_m, \mathcal{B}_m)_{1,u}, (\mathcal{Q}_{ml}, \mathcal{B}_m)_{u+1,s_l}\end{matrix}\right]. \tag{3.5}$$

Corollary 3.5. *Further setting $f_l = 1$ and $\wp = 1$ in (3.1), then, according to Srivastava [31], the incomplete H-function has the following image formula:*

$${}^{\Gamma}H^{u+1,v}_{r+1,\, s+1}\left[\varrho\middle|\begin{matrix}(\Theta_1, \mathfrak{E}_1 : z), (1+\varrho; \varrho_1), (\Theta_m, \mathfrak{E}_m)_{2,v} \\ (\varrho, \varrho_1), (\mathcal{Q}_m, \mathcal{B}_m)_{1,u}\end{matrix}\right]$$
$$= \frac{\tau^{\vartheta-1}\varphi}{\Gamma(\vartheta+1)}\left(\alpha - \frac{\tau\varphi}{(1+\vartheta)}\right){}^{\Gamma}H^{u+1,v}_{r+1,\, s+1}\left[\varrho\middle|\begin{matrix}(\Theta_1, \mathfrak{E}_1 : z), (1+\tau, \tau_1), (\Theta_m, \mathfrak{E}_m)_{2,v} \\ (\tau, \tau_1), (\mathcal{Q}_m, \mathcal{B}_m)_{1,u}\end{matrix}\right]$$
$$+ \Lambda\,{}^{\Gamma}H^{u,v}_{r,\, s}\left[\varrho\middle|\begin{matrix}(\Theta_1, \mathfrak{E}_1 : z), (\Theta_m, \mathfrak{E}_m)_{2,v} \\ (\mathcal{Q}_m, \mathcal{B}_m)_{1,u}\end{matrix}\right]. \tag{3.6}$$

Corollary 3.6. *Then, we insert* $z = 0$, $f_l = 1$, *and* $\wp = 1$ *in* (3.1). *This yields the image formula for the H-function that Srivastava* (*see, [30], pp.* 10) *proposed:*

$$H^{u+1,v}_{r+1,\,s+1}\left[\varrho\left|\begin{matrix}(\Theta_1,\mathfrak{E}_1:0),(1+\varrho;\varrho_1),(\Theta_m,\mathfrak{E}_m)_{2,v}\\(\varrho,\varrho_1),(\mathcal{Q}_m,\mathcal{B}_m)_{1,u}\end{matrix}\right.\right]=\frac{\tau^{\vartheta-1}\varphi}{\Gamma(\vartheta+1)}\Big(\alpha-\frac{\tau\varphi}{(1+\vartheta)}\Big)$$
$$\times H^{u+1,v}_{r+1,\,s+1}\left[\varrho\left|\begin{matrix}(1+\tau,\tau_1),(\Theta_m,\mathfrak{E}_m)_{1,v}\\(\tau,\tau_1),(\mathcal{Q}_m,\mathcal{B}_m)_{1,u}\end{matrix}\right.\right]+\Lambda\,H^{u,v}_{r,\,s}\left[\varrho\left|\begin{matrix}(\Theta_m,\mathfrak{E}_m)_{1,v}\\(\mathcal{Q}_m,\mathcal{B}_m)_{1,u}\end{matrix}\right.\right]. \tag{3.7}$$

4. Graphical Discussion

The three-dimensional Figures 1, 2, and 3 provide a detailed visualization of how blood glucose levels (ϱ) evolve (τ) under different values of the fractional-order parameter (ϑ). These plots reveal key trends that help understand the intricate relationship between glucose dynamics and physiological conditions.

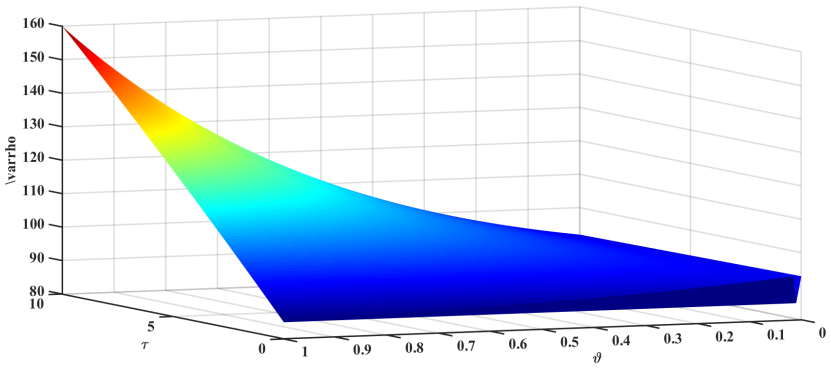

Figure 1. Variation of blood glucose level ϱ over time τ for different values of ϑ, with initial condition $\varrho(0) = 85$ and parameter $\varphi = 0.1$. The figure illustrates the impact of ϑ on glucose dynamics.

Along the x-axis, representing time (τ), distinct trends emerge in glucose regulation. At lower values of τ, blood glucose levels exhibit a smooth and gradual transition, indicating the body's ability to regulate glucose efficiently under stable conditions. However, as τ increases, fluctuations in glucose levels become more pronounced, reflecting the impact of metabolic processes such as insulin secretion, glucose absorption, and external factors like dietary intake and physical activity. These variations suggest that both internal physiological responses and external lifestyle factors influence long-term glucose regulation.

The fractional parameter ϑ along the y-axis significantly influences the rate of glucose variation. Lower values of ϑ produce smoother curves, suggesting a stable metabolic environment where glucose levels change gradually over time. In contrast, as ϑ approaches unity, the plots display more pronounced oscillations characterized by sharp peaks and troughs. This indicates a system with heightened sensitivity to metabolic fluctuations, where external stimuli, such as sudden changes in glucose intake or insulin response, have an immediate and pronounced effect.

These observations emphasize the complex interplay between glucose metabolism and fractional-order dynamics. The model effectively captures glucose regulation's memory and hereditary properties, highlighting how past glucose levels influence current states. This aspect is crucial in understanding conditions like diabetes, where delayed insulin responses or prolonged glucose retention can lead to metabolic instability. To ensure biological relevance, the parameter values in this study were selected based on established literature, which are described in Table 1. Where empirical data is unavailable, reasonable approximations are made while maintaining the model's generality. These choices allow the simulation of various metabolic scenarios, providing deeper insights into glucose homeostasis and potential strategies for managing metabolic disorders.

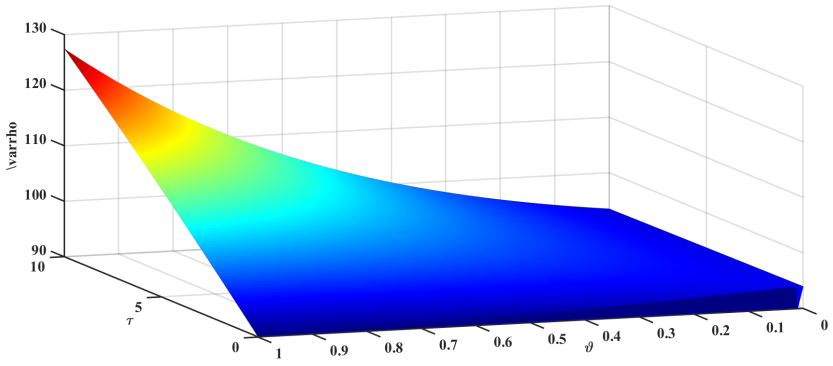

FIGURE 2. Variation of blood glucose level ϱ over time τ for different values of ϑ, with initial condition $\varrho(0) = 90$ and parameter $\varphi = 0.05$. The figure illustrates the effect of ϑ on glucose dynamics.

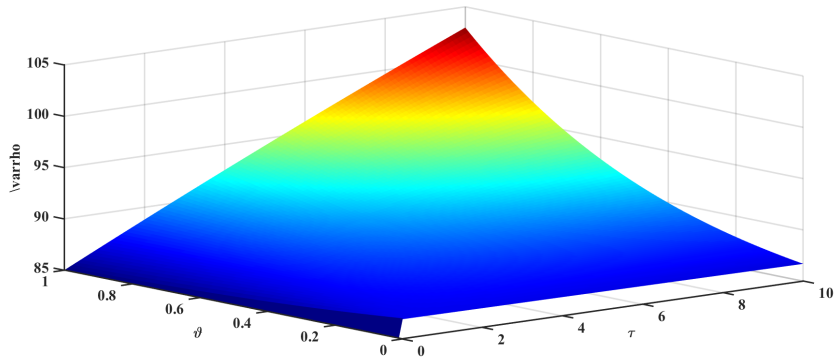

FIGURE 3. The variation of blood glucose level ϱ for different values of ϑ, considering the initial condition $\varrho(0) = 85$ and parameter $\varphi = 0.02$. The figure demonstrates the influence of ϑ on glucose regulation over time.

TABLE 1. Summary of Variables and Parameters.

Symbol	Description	Unit	Remarks
ϱ	Blood glucose concentration	mg/dL	Primary quantity analyzed
τ	Time	minutes	Defines temporal evolution of glucose levels
ϑ	Fractional-order parameter	Dimensionless	Captures memory effects
φ	Transfer coefficient	min^{-1}	Governs glucose removal rate
α	Baseline glucose level	mg/dL	Represents equilibrium glucose concentration
Λ	Initial blood glucose concentration	mg/dL	Constant at $\tau = 0$

Overall, this graphical analysis underscores the importance of fractional-order modeling in studying blood glucose regulation. By integrating these findings, the study offers valuable perspectives for medical research, particularly in optimizing treatment strategies for diabetes and other metabolic diseases.

5. Conclusion

This study successfully establishes a mathematical framework for glucose dynamics in human blood using the incomplete ℵ-function, demonstrating its effectiveness in capturing complex glucose regulation mechanisms. A key outcome of this work is the ability to generalize multiple glucose behavior patterns by adjusting fractional-order parameters and transfer coefficients, offering a more flexible and accurate representation of glucose metabolism. The results indicate that fractional-order modeling provides deeper insights into glucose regulation's memory effects and hereditary properties, which are often overlooked in classical models. Furthermore, the quantitative analysis highlights critical threshold values that influence glucose homeostasis, potentially aiding in the early detection and management of metabolic disorders such as diabetes. While the complexity of parameter estimation poses a challenge, the model's predictive capability and adaptability make it a valuable tool for advancing research in medical science, applied mathematics, and biochemical analysis. Future work may focus on experimental validation and refining parameter estimation techniques to enhance the model's applicability.

Acknowledgment: The author is grateful to the editors and reviewers for their valuable and constructive comments, which have significantly improved the quality of this manuscript.

Funding: This study received no specific financial support.

Data Availability: No data was used for the research described in the article.

Declaration of Competing Interest: The author declares that they have no known competing financial interests or personal relationships that could have appeared to influence the work reported in this paper.

References

[1] W. Adel, H. Günerhan, K. S. Nisar, P. Agarwal, and A. El-Mesady, *Designing a novel fractional order mathematical model for COVID-19 incorporating lockdown measures*, Sci. Rep., *14*(1) (2024), 2926.

[2] V. Agarwal, M. C. Khatumariya, Shyamsunder, and S. Kumar, *Internal blood pressure dynamics: modeling with incomplete ℵ-function and fractional operator*, Adv. Math. Sci. Appl., *34*(02) (2025), 651–662.

[3] D. Albayrak, S. D. Purohit, and U. Faruk, *Certain inversion and representation formulas for q-Sumudu transforms*, Hacet. J. Math. Stat., *43*(5) (2014), 699–713.

[4] M. K. Bansal and D. Kumar, *On the integral operators pertaining to a family of incomplete I-functions*, AIMS Math., *5*(2) (2020), 1247–1259.

[5] M. K. Bansal, D. Kumar, K. S. Nisar, and J. Singh, *Certain fractional calculus and integral transform results of incomplete ℵ-functions with applications*, Math. Methods Appl. Sci., *43*(8) (2020), 5602–5614.

[6] S. Bhatter, Nishant, Shyamsunder, and S. D. Purohit, *Srivastava-Luo-Raina M-transform involving the incomplete I-functions*, Comput. Methods Differ. Equ., *12*(1) (2024), 159–172.

[7] S. Bhatter, K. Jangid, S. D. Purohit, and Shyamsunder, *Determining glucose supply in blood using the incomplete I-function*, Differ. Equ. Appl. Math., *10* (2024), 100729.

[8] S. Bhatter, S. D. Purohit, and Shyamsunder, *Several computational based expansions for incomplete ℵ-function using the Leibniz rule*, In International Conference on Mathematical Modelling, Applied Analysis and Computation, *953* (2023), 306–314.

[9] D. S. Bodkhe and S. K. Panchal, *On Sumudu transform of fractional derivatives and its applications to fractional differential equations*, Asian J. Math. Comput. Res., *11*(1) (2016), 69–77.

[10] M. A. Chaudhry and S. M. Zubair, *On a class of incomplete gamma functions with applications*, Chapman and Hall/CRC, 2001.

[11] A. El-Mesady and H. M. Ali, *The influence of prevention and isolation measures to control the infections of the fractional chickenpox disease model*, Math. Comput. Simul., *226* (2024), 606–630.

[12] A. El-Mesady, A. Elsadany, A. Mahdy, and A. Elsonbaty, *Nonlinear dynamics and optimal control strategies of a novel fractional-order lumpy skin disease model*, J. Comput. Sci., *79* (2024), 102286.

[13] A. El-Mesady, O. J. Peter, A. Omame, and F. A. Oguntolu, *Mathematical analysis of a novel fractional order vaccination model for tuberculosis incorporating susceptible class with underlying ailment*, Int. J. Model. Simul. (2024), 1–25.
[14] A. Elsonbaty, M. Alharbi, A. El-Mesady, and W. Adel, *Dynamical analysis of a novel discrete fractional lumpy skin disease model*, Partial Differ. Equ. Appl. Math., *9* (2024), 100604.
[15] M. Higazy, S. A. Alsallami, S. Abdel-Khalek, and A. El-Mesady, *Dynamical and structural study of a generalized Caputo fractional order Lotka-Volterra model*, Results Phys., *37* (2022), 105478.
[16] K. Jangid, S. Bhatter, S. Meena, D. Baleanu, A. M. Qurashi, and S. D. Purohit, *Some fractional calculus findings associated with the incomplete I-functions*, Adv. Difference Equ., *2020*(1) (2020), 265.
[17] K. Jangid, S. D. Purohit, K. S. Nisar, and T. Shefeeq, *The internal blood pressure equation involving incomplete I-functions*, Inf. Sci. Lett., *9*(3) (2020), 2.
[18] H. Kang, K. Han, and M. Choi, *Mathematical model for glucose regulation in the whole-body system*, Islets, *4*(2) (2012), 84–93.
[19] J. N. Kapur, *Mathematical models in biology and medicine*, Affiliated East-West Press Pvt. Ltd., New Delhi, India, 1985.
[20] A. A. Kilbas, H. M. Srivastava, and J. J. Trujillo, *Theory and applications of fractional differential equations*, Elsevier, 2006.
[21] S. Panwar, R. M. Pandey, S. D. Purohit, and Shyamsunder, *A mathematical analysis of non-linear smoking model via fractional operators*, Comput. Methods Differ. Equ. (2024), 1–22.
[22] A. K. Rathie, *A new generalization of generalized hypergeometric functions*, Le Math., *LII* (1997), 297–310.
[23] D. Sanyal and A. Maiti, *Stochastic variation of concentration in blood glucose*, Appl. Sci. Periodical, *2* (1999), 65–67.
[24] V. P. Saxena, *Formal solution of certain new pair of dual integral equations involving H-functions*, Proc. Nat. Acad. Sci. India Sect. A, *52* (1982), 366–375.
[25] Shyamsunder, *Comparative implementation of fractional blood alcohol model by numerical approach*, Crit. Rev. Biomed. Eng., *53*(2) (2024), 11–19.
[26] Shyamsunder, Kritika, and S. D. Purohit, *Expansion formulae for incomplete Yang-Yu-W-function with Bessel function*, Commun. Calc. Anal. Spec. Funct. Math. Phys., *1*(1) (2024), 03–10.
[27] Shyamsunder and S. D. Purohit, *Generalized Eulerian integrals involving the incomplete I-function*, Adv. Math. Sci. Appl., *34*(1) (2025), 301–311.
[28] Shyamsunder, *Solutions of fractional kinetic equation involving incomplete ℵ-function*, In International Conference on Computational Modeling and Sustainable Energy (2025), 215–230.
[29] Shyamsunder and D. Gangwar, *Impact of fractional order on reaction rates: Solutions to kinetic equations with incomplete ℵ-function*, Comput. Methods Differ. Equ. (2025), 1–9.
[30] H. M. Srivastava, K. C. Gupta, and S. P. Goyal, *The H-functions of one and two variables, with applications*, South Asian Publishers, 1982.
[31] H. M. Srivastava, R. K. Saxena, and R. K. Parmar, *Some families of the incomplete H-functions and the incomplete $\bar{H}$-functions and associated integral transforms and operators of fractional calculus with applications*, Russ. J. Math. Phys., *25*(1) (2018), 116–138.
[32] N. Südland, B. Baumann, and T. F. Nonnenmacher, *Who knows about the ℵ-function*, Fract. Calc. Appl. Anal, *1*(4) (1998), 401–402.
[33] N. Südland, G. Baumann, and T. F. Nonnenmacher, *Fractional driftless fokker-planck equation with power law diffusion coefficients*, In Computer Algebra in Scientific Computing CASC 2001, pages 513–528, Springer, 2001.
[34] R. Walker and J. R. Type, *Diabetes–your questions answered*, Dorling Kindersley, 2006.
[35] D. H. Wasserman, *Four grams of glucose*, Am. J. Physiol., *296*(1) (2009), E11–E21.